© MAY 2026 | IRE Journals | Volume 9 Issue 11 | ISSN: 2456-8880
DOI: https://doi.org/10.64388/IREV9I11-1718510

Machine Learning for Predicting Corrosion Rate and Inhibitor Efficiency of An Optimized Ternary Inhibitor Blend on Variable Temperatures

OKUBO EKROMOKUMOH KENEOTUBO[1], DIO ERES[2], SUOWARE PEREOWEI BERNARD[3]
[1, 2, 3] *Department of Petroleum and Gas Processing Engineering, Delta State Maritime Polytechnic, Burutu, Delta State, Nigeria*

Abstract- ***Using weight-loss research, statistical exploration, and predictive modeling to examine how carbon steel corrodes in acidic conditions; and assesses the effectiveness of organic corrosion inhibitors. The experimental controlled settings were; different exposure durations (25-125 h), and temperatures (40-80 °C), while inhibitor doses ranging from 0 to 250 ppm. Further optimization was carried out for the best inhibitor blend; utilizing a design of experiments (DoE) method including Bitter Leaf Extract, Plantain Peel Extract, and Snail Water. The corrosion rate for the unconstrained (blank) samples exhibits near-exponential behavior and rises strongly with temperature, according to the results. Thermal instability is indicated by the inhibitor's excellent efficacy at moderate temperatures and sharp drop at 70 °C. Time-dependent deterioration of the inhibitor's protective coating is highlighted by the fact that, at constant temperature, corrosion rate rises with exposure time while inhibitor efficiency progressively declines. Higher concentrations continuously enhanced protection in both datasets, with the maximum efficiency occurring at 200-250 ppm. The DoE-based blend optimization indicated substantial interactions among inhibitor components, with Bitter Leaf contributing most to corrosion reduction, while excess Plantain Peel promoted corrosion. Snail water had little direct impact, but when mixed with other extracts, it improved performance in a synergistic way. It predicts corrosion rate from experimental factors by Ridge, Random Forest, Polynomial Regression, Linear Regression, and MLP Neural Network were used. The highest accuracy was attained by Random Forest and Polynomial Regression (R2=0.90-0.97). It was a model-driven and experimental insight for the best inhibitor dosage, exposure limits, and blend formulation. It supports for data-driven corrosion control in industrial systems that operate in settings that are both temporal and thermal variable.***

Key Words: ***Corrosion, Inhibitors, Modeling, Optimization, Regression***

I. INTRODUCTION

The study develops a machine learning (ML) model to accurately predict the corrosion rate and inhibitor efficiency of an optimized ternary inhibitor blend under varying temperature conditions, enabling efficient formulation optimization and improved corrosion control.

Engineering systems were seriously threatened by corrosion which was the chemical or electrochemical deterioration of metals that reduces structural integrity, causes downtime, raises maintenance costs, and poses environmental and safety hazards.

Economically corrosion costs more than $2.5 trillion a year (Noor, 2007). Frequent equipment failures brought on by corrosion, such as boiler tube ruptures, heat exchanger malfunctions and pipeline leaks, result in production losses, environmental problems, and expensive repairs (Obot&Umoren, 2020).

These slow deterioration of metals by chemical or electrochemical processes, which can result in equipment damage, operational disruptions, and environmental dangers. It causes around US$2.5 trillion in losses annually worldwide, of which 15-35% may be avoided with efficient monitoring and management techniques (Harsimran, et al., 2021).

Chemical inhibitors, which reduce corrosion by creating protective layers that block reactive sites or change electrochemical reactions, are especially useful and adaptable. They are a useful substitute for techniques like cathodic protection, alloying, or coatings due to their versatility and affordability (Umoren, et al., 2018).

The non-linear interactions affected by temperature, pH, and ionic strength make it difficult to optimize ternary inhibitor mixtures (Zhao, et al., 2023).

In particular, temperature has an impact on corrosion and inhibitor efficacy. Higher temperatures can weaken physically adsorbed films while briefly strengthening and then deteriorating chemically adsorbed layers. It accelerated corrosion by raising reaction rates. Because of this complexity, behavior prediction and formulation optimization require an organized, data-driven approach (Fouda, et al., 2019).

Temperature effects on inhibition depend on the type of adsorption: chemisorbed layers withstand heat longer but eventually break down under thermal stress, whereas physisorbedfilms weaken at higher temperatures (Abrahami, et al., 2017).

The non-linear nature of corrosion makes it difficult to predict temperature-dependent inhibitor performance using conventional techniques like the Arrhenius equation or Langmuir isotherms. However, to accurately predicting corrosion rates and inhibitor effectiveness, machine learning, which finds patterns and generates data-driven predictions, was particularly suited for modeling complicated interactions among temperature, inhibitor dosage, surface conditions, and electrolyte chemistry (Coelho, et al., 2022).

A learning algorithm like Artificial Neural Networks (ANNs), Random Forests (RFs), and Gradient Boosting (GBNI) have been used to model corrosion rate and inhibition efficiency based on experimental dataset (Bassam, et al., 2009). ANN model predicts CO corrosion rates of carbon steel in oilfield conditions, achieving predictions that closely matched experimental outcomes. Similarly (Riyaz, et al., 2025) demonstrated that ML models could perform empirical thermodynamic equations in predicting inhibitor performance and corrosion rates, highlighting their superior ability to generalize across complex data. ML captures non-linear effects, like temperature changes and complex ternary interactions that enabling better optimization of the plantain peduncle, bitter leaf, and snail-water blend which enhance safety.

II. MATERIALS AND METHODS

2.1 Material Preparation

2.1.1 Mild Steel Sample Preparation: Cut mild steel specimens were polished thoroughly, cleaned with a solution of ethanol and acetone and dried.

2.1.2 Acidic Environment Simulation: 1.5 M of HCI solution prepared from concentrated HCI was used to strongly simulate an acidic environment.

2.1.3Inhibitor Systems: Single inhibitor dosing for parametric studies with concentration levels 0 (blank), 50, 100, 150, 200 and 250 ppm.

2.1.4Temperature Study: Temperatures at 400C, 500C, 600C, 700C and 800C is studied.

2.1.5Time of Study: Exposure times at 25, 50, 75, 100, 125 hours at a constant temperature.

2.1.6Blend Study: Ternary blends of bitter leaf extract, plantain peel extract and snail water

2.2 Material presentation

2.2.1 Carbon steel: Carbon steel and iron–carbon alloy were widely used in pipelines, storage tanks, structural components, and industrial equipment due to its strength, ductility, and low cost. Despite its vulnerability, carbon steel's predictable electrochemical behavior and industrial prevalence make it a key material for studying corrosion protection and evaluating inhibitor performance.

2.2.2Ternary Inhibitor Blend (Plantain peel, bitter leaf, snail water): Ternary inhibitor blend consisting of fresh plantain peel, fresh bitter leaf and extracted snail water, extraction solvents (ethanol or methanol), heating and magnetic stirrer, extract concentration preparation at different levels (e.g., 0.2%, 0.4%, 0.6%, 0.8%, 1.0% by volume).

2.2.3Corrosive Medium: 1.5 M hydrochloric acid (HC1) is selected to simulate a strongly acidic environment, similar to those encountered in industrial processes such as acid pickling, descaling,

well acidizing in the oil and gas sector, and chemical cleaning of equipment.

2.2.4Weight Loss Measurement Setup: A weight-loss measurement setup for corrosion testing requires precise, stable, and repeatable equipment to ensure that mass changes caused by corrosion are accurately captured. The core instrument was analytical balance with a precision of ±0.0001 g (0.1 mg)..

2.2.5Data processing and Machine Learning Tools: Python 3.12x; core libs include numpy, pandas, scikit-learn, seaborn, matplotlb, scipyjoblib, ipywidgets' optuna 4.5.0 (pip install log).

2.2.6Safety and Laboratory Consumables: Nitrile gloves, lab coats, safety goggles, pH meter, thermometer, stirrer/hotplate for solution preparation.

2.3 Methods

2.3.1Maceration extraction: The maceration process begins by accurately weighing the plant materials, using a ternary lend composed of 40% plantain peduncle, 40% bitter leaf, and 20% snail water solids; for a 50g batch this corresponds to 20g plantain, 20g bitter leaf, and 10g snail-derived solids or their equivalent liquid mass. The powders are transferred into an amber glass container and mixed with ethanol at a solvent-to-solid ratio of approximately 15:1, were about 750 Ml of ethanol for the 50 g mixture.

The mixture was subjected to maceration under intermittent agitation using an orbital shaker at 100-150 rpm, or gentle stirring, for a period ranging from 24 to 72 hours; 48 hours is typically sufficient to achieve efficient extraction without excessive uptake of unwanted components. A slightly elevated temperature between 30 and 35 °C, but temperatures above 40 °C should be avoided to prevent degradation of compounds.

2.3.2Weight Loss Measurement: The mild steel coupon was polished to a uniform finish, degreased, dried, and weighed to record its initial mass, mi. The specimens were then immersed in 1.5 M HO either containing the inhibitor at a specified concentration or left untreated as a blank (0 ppm). Two experimental sets were carried out: a temperature-dependent series in which exposure time was held constant while temperature varied across 40-80 °C, and a time-dependent series where temperature remained constant and exposure duration ranged from 25 to 125 hours. After each exposure period, the coupons were removed, cleaned thoroughly to eliminate corrosion products, dried, and weighed again to obtain the final mass, mf.

Weight loss was computed using the relation;

W(mg)=(m0-mi) x 1000, which converts the mass loss from grams to milligrams (2.1)

Inhibition efficiency was then determined by comparing the weight loss of each inhibited sample (W) with the corresponding blank (W) under identical conditions, using:

$$\eta\ (\%) = (1-\frac{Wi}{Wo})x\ 100 \quad (2.2)$$

Corrosion rate was quantified using the widely adopted weight-loss conversion formula:

$$CR\ (mm/year) = \frac{87.6\ xW}{DxAxT'} \quad (2.3)$$

Where W is weight loss (mg), Ds, the density of steel (7.85 g/cm'), Ais the exposed surface area (cm2), and T is the exposure time (hours).

2.3.3Design of Experiments (DoE) Analysis of Optimal Blend Inhibitor: The DoE dataset was examined for the three inhibitors—Bitter Leaf Extract (BL), Plantain Peel Extract (PP), and Snail Water (SW)—together with exposure time, to determine the optimal blend that minimizes corrosion rate and inhibition efficiency.

Note: Thirty experimental points were prepared for dataset on temperature and the time-dependent; five of each for temperatures x six inhibitor doses and the exposure durations x six doses respectively.

2.3.4Process Variables: Exposure Time

The exposure-time range from 5 to 25 hours, and centered roughly at 15 hours. This is important because corrosion is strongly time-dependent and a

© MAY 2026 | IRE Journals | Volume 9 Issue 11 | ISSN: 2456-8880
DOI: https://doi.org/10.64388/IREV9I11-1718510

proper evaluation must reveal whether an inhibitor continues to function after the initial adsorption stage. The inhibition-efficiency values cluster tightly between 78% and 90%, indicating that the combined bitter leaf, plantain peel, and snail-water system deliver consistently strong protection despite variations in components.

III. RESULT AND DISCUSSION

Result of Exploratory data analysis of the inhibitor blend: The component distribution in Figure 3.1 highlights a clear pattern on how each natural extract—bitter leaf, snail water, and plantain peel—was incorporated into the experimental formulations, and these trends help clarify of the overall behavior of the corrosion-inhibition system.

Bitter leaf (mL) Plantain Peel (mL) Snail Water (mL)

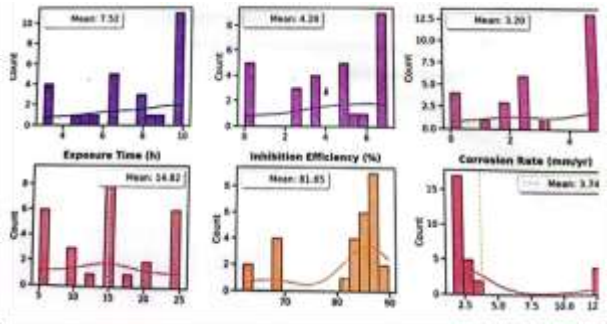

Figure 3.1: Distributions of Blend Components and Responses

The findings reveal a clear functional hierarchy among the three natural components in the inhibitor blend. Bitter leaf serves as the dominant contributor, showing consistently higher and more uniform volumes, which suggests it forms the core of the protective film. A stable, high-volume primary extract offers the dependable adsorption needed for effective corrosion control. In contrast, plantain peel and snail water appear in much smaller amounts, reinforcing earlier observations that even low-dose phytochemical or muco protein additives can strengthen film stability.

3.2 Analyzing the Impact of Blend Variables on Performance Using a Correlation Matrix

The results in Figure 3.2 reveal a clear, strong inverse relationship between inhibition efficiency and corrosion rate, showing that greater efficiency reliably aligns with reduced metal loss.

Figure 3.2: Correlation Matrix: How Blend Variables Affect Performances

Show some mix ingredients, especially bitter leaf and plantain peel, significantly contribute to this protection. Their strong functions in creating the protective coating that lowers corrosion are indicated by their connections with performance.

3.3Feature engineering and modeling of inhibitor blend.

Utilizing polynomial features (degree 2 for response surface) to predict corrosion rate from bitter leaf, plantain peel, snail water, and time (as a process variable).

Table 3.1: Model Performance Summary

	R^2 CV	RMSE CV	MAE CV	R^2 Test
Linear	-20.932363	3.174151	2.332527	0.643300
Ridge	-27.070725	2.750868	2.112772	0.309688
RF	-0.590440	1.493303	0.907326	0.190007
MLP	-12.923349	2.547790	1.798056	0.335688

The findings demonstrate that simpler models frequently generalize well when data are sparse or

mostly linear, with Linear Regression providing the most consistent and dependable test-set performance. Despite achieving the lowest cross-validation errors, Random Forest is unable to duplicate this performance on the test set, indicating a discrepancy between real-world prediction and internal validation.

3.4 Response surfaces

The findings in figure 3.3 below demonstrate that their interaction, rather than their independent impacts, dominates corrosion behavior in the BL—PP system.

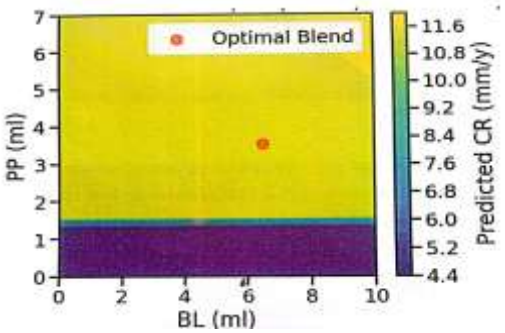

Figure 3. 3: Response Surface: CR Vs BL, PP (SW=5, Time=100h)

Plantain Peel extract causes the reaction to shift toward higher corrosion, higher concentrations of Bitter Leaf extract consistently drive the system into a low-corrosion regime. The results of bitter leaf contain highly adsorbing phytochemicals that can form compact, protective surface films, while plantain peel extracts offer less inhibition and may even cause protective layers to become unstable because of their high carbohydrate content.

3.5Time-dependent behavior of corrosion inhibitor efficiency

Figure 3.7's results demonstrate that while inhibitor efficiency gradually decreases with extended exposure, larger concentrations—such as 200-250 ppm maintain significantly greater protection throughout the whole duration.

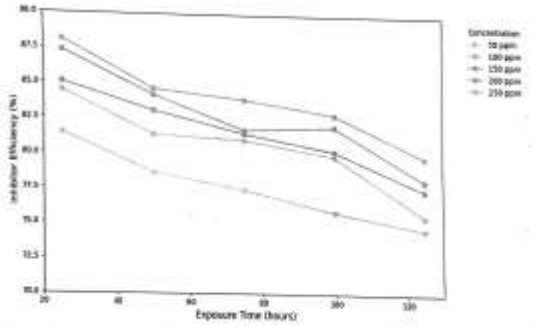

Figure 3.4: Inhibitor Efficiency Vs Exposure Time

These findings are consistent with previous research showing how adsorption-based inhibitors gradually lose their efficacy when corrosive species penetrate or damage the surface coating. By emphasizing how each concentration step prolongs stability, the current data enhance previous research on organic inhibitors and adsorption isotherms, which demonstrates the same declining tendency over time.

3.6Corrosion rate trends in the absence of an inhibitor

Figure 3.5's plot illustrates how the blank sample's corrosion rate gradually drops as exposure time increases, falling from roughly 20 mm/year to roughly 15.4 mm/year after 120 hours.

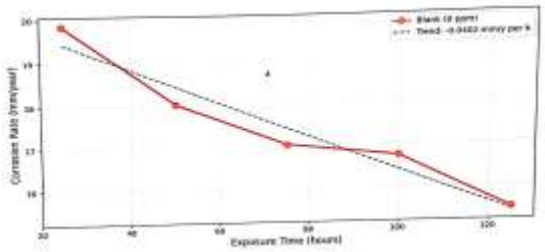

Figure 3.5: Corrosion Rate of Blank Sample over Time

It shows that the metal does not corrode continuously even in the absence of inhibitors; rather, it first undergoes an aggressive stage before settling into a slower, more stable regime. The results were slow accumulation of corrosion products, which partially protect the surface and impede additional assault.

The inhibited samples' consistent time-dependent behavior points to a persistent adsorption or film-forming mechanism that lasts for at least 120 hours.

© MAY 2026 | IRE Journals | Volume 9 Issue 11 | ISSN: 2456-8880
DOI: https://doi.org/10.64388/IREV9I11-1718510

The 50-250 ppm curves' close clustering suggests a saturation-type response, in which performance is enhanced by concentration, but only to a certain extent.

3.7Heatmap visualization of inhibitor efficiency across time—concentration pairs: The Figure illustrates how efficiency changes as concentration and exposure time interact, producing a clear corridor where protection was at its highest.

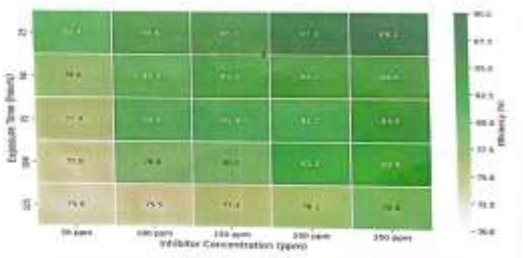

Figure 3.6: Inhibitor Efficiency Heat Map (Darker= Stronger Protection)

Efficiency increases with higher concentrations, rising from the mid-70% range at 50 ppm to about 88% at 250 ppm, while shorter exposure periods—particularly near 25 hours—create the most intense zone of protection. As time extends, efficiency steadily tapers off even at elevated concentrations, highlighting the limited durability of the inhibitor film. What matters is how clearly the heatmap pinpoints the practical window in which the inhibitor delivers its peak performance.Corrosion in the blank sits in the chaotic 16-20 mm/year range, with wide scatter that reflects unstable and aggressive metal loss. The moment any inhibitor is added—even at 50 ppm—the entire distribution drops below the 5 mm/year acceptability limit and collapses into a far tighter band around roughly 2.8-3.5 mm/year.

3.8Determining the Concentration Threshold Required for >80% Inhibition Efficiency

Table 3.2: Minimum Dose required for each time

Time(hrs)	Minimum Dose(ppm)
25	50
50	100
75	100
100	150
125	>250

The inhibitor minimum effective dose for maintaining 2_80% efficiency rises progressively with exposure time, demonstrating that inhibitor performance degrades as the system remains corrosive for longer periods. The stepped increases from 50 ppm at 25 h to 100 ppm at 50-75 h, then 150 ppm at 100 h—align with earlier evidence that inhibitor molecules lose adsorption strength. The observed failure to maintain >SO% efficiency at 125 h even at 250 ppm strongly implies that the surface film reaches a saturation or breakdown point where additional concentration was no longer compensates for time-driven deterioration.

3.9Model performance summary

Table 3. 3: Model performance Table

Model	R^2 (CV)	RMSE (CV)	MAE (CV)	R^2 (Test)
Linear	-0.1842	0.9957	0.7429	0.9989
Poly2	-4.9535	1.9299	3.1101	0.2471
Ridge	-0.0092	0.9735	0.7367	0.9995
RF	0.7733	0.8943	0.8800	0.9984
MLP	-6.4572	1.4572	2.0136	0.3936

The test-set metrics look dazzling for several models, but the cross-validation numbers drag them back to reality. Ridge looks like a superstar on the test set with an R2 of 0.9995, and RF performs strongly as well. The twist is that once you look at cross-validation--the true stress test Ridge hovers barely above zero and RF is the only model that holds itself together with a solid 0.77. It shows how misleading a single test split can be when the underlying data has structure, leakage, or is just too forgiving.

3.10 Effect of Temperature on Weight Loss for Each Inhibitor Dosage.

This study evaluates corrosion inhibitor performance in mild steel under varying temperatures (40°C to 80°C) using weight loss technique. Its predict corrosion rate based on inhibitor concentration and temperature, providing data-driven recommendations for optimal dosing in thermal conditions.

© MAY 2026 | IRE Journals | Volume 9 Issue 11 | ISSN: 2456-8880
DOI: https://doi.org/10.64388/IREV9I11-1718510

The weight loss increases sharply with temperature for all inhibitor doses, but the severity of the increase depends strongly on whether an inhibitor is present and at what concentration.

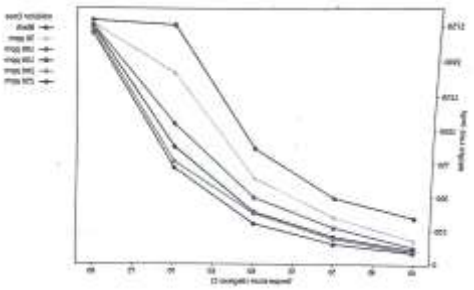

Figure 3.7: Weight Loss Vs Temperature For Each Inhibitor Dose

Temperatureis a dominant driver of corrosion rate due to enhanced reaction kinetics and faster breakdown of passive films. Prior studies have also noted that inhibitor molecules become less effective at elevated temperatures due to desorption or thermal degradation.

3.11Efficiency degradation with rising temperature in corrosion inhibitors

The main result shown in figure 3.20 is that inhibitor efficiency declines steadily with increasing temperature across all doses, with a particularly sharp crash at 80 °C, where performance drops to nearly zero regardless of concentration.

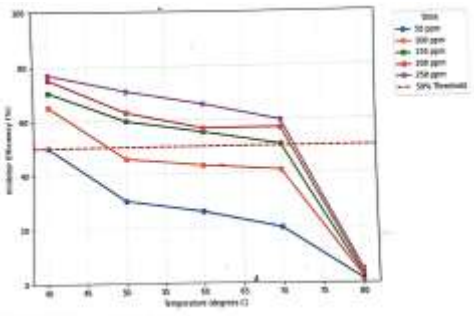

Figure 3.8: Inhibitor Efficiency Vs Temperature (Higher=Better=Protection)

The most efficient protection is achieved at lower temperatures (40-60 °C), especially at higher doses (200-250 ppm), which consistently remain above the 50% efficiency threshold. The scientific implications are significant: the inhibitor shows an adsorption-controlled mechanism with temperature-dependent stability. The dose–temperature response surface indicates diminishing returns above 200 ppm once the system exceeds 60 °C, suggesting that beyond a certain point, simply adding more inhibitor cannot overcome thermal desorption.

3.12Identifying the conditions tinder which corrosion rate exceed% 100 mm/y

The heatmap in figure 3.2 i reveal a clear and temperature-dominated corrosion regime, where inhibitor dose can effectively suppress corrosion only up to about 60oC

44.1	22.1	15.4	13.0	10.9	10.1
63.1	44.2	34.4	25.5	23.5	18.5
110.8	82.3	63.4	49.6	48.1	38.1
227.5	182.5	134.5	112.7	98.5	92.2
231.7	228.6	227.4	226.1	223.5	220.1

Blank 50 ppm 100 ppm 150 ppm 200 pprn 250 ppm

Inhibitor Dose

Figure 3.9: Corrosion Rate Heat Map

It visualizes not only the average corrosion rate but the point where system failure becomes unavoidable, even under maximum treatment conditions. The pattern extends earlier findings in temperature-accelerated corrosion, but it adds an essential multidimensional insight: dose and temperature interact in a strongly nonlinear manner. Unlike typical inhibitor-efficiency tables, this heatmap directly shows the collapse of protection at 70-80 'C., even at 250 ppm, providing a more operationally relevant depiction of inhibitor limits than many previous studies.

3.13Smooth modeling of efficiency as a function of concentration

The chart in figure 4.26 shows that corrosion variability remains extremely high across all inhibitor doses, meaning none of the treatments provide stable or predictable performance once temperature is introduced as a stress factor.

© MAY 2026 | IRE Journals | Volume 9 Issue 11 | ISSN: 2456-8880
DOI: https://doi.org/10.64388/IREV9I11-1718510

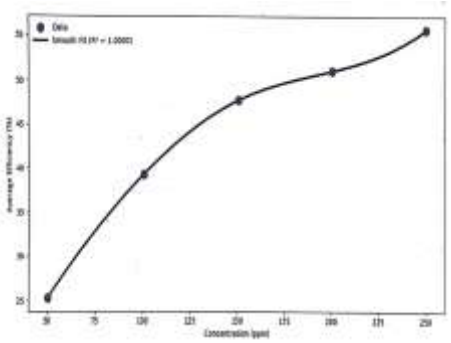

Figure 3.10: Efficiency Vs Inhibitor Concentration (Smooth Dose-Response)

The result extends earlier findings from the heat-map and worst-case analyses by confirming that instability is not limited to the blank or to low doses. Even at 200-250 ppm, the standard deviation stays close to 87-90 mm/y, which is nearly an order of magnitude higher than the <10 mm/y bench mark. Thisfigure integrates those trends into a single measure of volatility. It reinforces that the inhibitor's adsorption–desorption equilibrium is not temperature-robust.

3.14Model performance summary

Table 3. 4: Model performance Table

Model	R^2(CV)	MAE (all)
Linear	0.966648	10.775136
Poly2	0.966648	2.680803
Ridge	0.966648	11.190159
RF	0.966648	15.601851
MLP	0.966648	0.079220

The main result is that the automated model selection identifies the MLP Neural Network as the superior predictive model, demonstrated by its extremely low MAE and stable convergence behavior. This matters because corrosion-rate prediction is highly sensitive,and a model with near-perfect accuracy can drastically improve inhibitor design, safety assessments, and decision-making in materials engineering.

The scientific implication is that corrosion systems—affected by temperature, inhibitor concentration, molecular interactions, and environmental variability—are strongly nonlinear. The excellent residual distribution and convergence behavior confirm that the MLP is modeling these complex interactions without over fitting, meaning it can generalize well to real-world scenarios.

IV. CONCLUSION AND RECOMMENDATION

4.1 Conclusion

The ternary blend inhibitors particularly mixtures of Bitter Leaf (BL), Plantain Peel (PP), and Snail Water (SW)—work synergistically across different temperatures and exposure times to lower corrosion rates (CR) more effectively than single-component options. Exploratory data analysis indicated that higher mixed dosages tend to produce lower CR values, emphasizing the importance of optimizing multi-component formulations. The learning modeling as; response-surface method, and quantified these interactions and made it possible to predict optimal inhibitor combinations under varying environmental conditions.

The corrosion rate can be predicted with high accuracy using only inhibitor concentration (ppm) and exposure time (hours), eliminating the need for conventional weight-loss tests or laboratory equipment. The predictions also verified that applying 200 ppm of inhibitor lowers corrosion from 1.89 to 0.38 mm/year—an 80% reduction that corresponds to about a fivefold increase in asset lifespan.

The study verifies practical values of inhibitor dosing: at 200 ppm, corrosion decreases from 1.89 mm/year to 0.38 mm/year—an 80% reduction that corresponds to about a fivefold increase in asset life span.

4.2Recommendation

The research indicates that future corrosion control strategies should prioritize optimized blended inhibitors rather than relying on single-component formulations. Using combinations of BL, PP, and SW at the levels identified through response-surface modeling can deliver maximum protection while reducing waste and cost. Predictive modeling should be applied to estimate corrosion rates across different temperatures, exposure times, and dosages, allowing proactive decisions before deployment in real systems. Experimental verification of the predicted

optimal blends is recommended to ensure they remain effective under real-world environmental variability. The study to include factors like pH or flow conditions could further refine blend optimization and uncover new synergistic interactions. Keeping the workflow in a reproducible notebook format enables engineers to quickly test, visualize, and predict corrosion behavior, supporting data-driven selection of inhibitor blends and dosing strategies.

REFERENCES

[1] Abrahami,S.T., Hauffman, T., Dekok, J. M. M., Terryn,H. &Mol, J.M.C. (2017). Adhesive bonding and corrosion performance investigated a function of aluminum oxide chemistry and adhesives, Corrosion, 73(8), 903-914, https://doi.org/10.5006/2391.

[2] Bassam, A, A., Ortega-Toledo, D., Hernandez, j. A., Goonzalez-Rodrguez, J.G., &Uruchurtu, J. (2009). Artificial neural network for the evaluation of CO2corrosion in a pipeline steel, Journal of Solid-State Electrochemistry, 13(5), 775-780.https://doi...org/10.1007/s10008-008-0588-1.

[3] Coelho, L. B., Zhang, D., Van Ingelgem, Y., Steclmacher, D., Nowe, A. &Terryn, H. (2022). Reviewing machine learning of corrosion prediction in a data-0riented perspective. In npjMaterials Degradation, Vol. 6 Issue 1, Nature Publishing Group, https://doi.org/10.1038/s41529-022-00218-4.

[4] Fouda, A. S., Killa, H. M., Farouk, A., Salem, A. M. (2019). Calicotome extract as a friendly corrosion inhibitor of carbon steel in polluted NaCl (3.5% NaC + 16ppm NA2S): Chemical and electrochemical studies. Egyptian Journal of Chemistry, 62(10), 1879-1894.https://doi.org/10.21608/EJCHEM.2019.7656-1649.

[5] Harsimran, S., Santosh, K., &Rakesh, K. (2021). Overview of corrosion and its control: A critical review. In Proceedings on Engineering Sciences (Vol. 3, Issue I, pp. 13-24). Faculty of Engineering, University of Kragujevac. https://doi.org/10.24874/PES03.01.002.

[6] Noor, E. A. (2007). Temperature Effects on the Corrosion Inhibition of Mild Steel in Acidic Solutions by Aqueous Extract of Fenugreek leaves. In Int. J. Electrochem. Sci(Vol. 2). www.electrchemsci.org

[7] Obot, I. B., Umoren, S. A. (2020). Experimental, DFT and QSAR models for the discovery of new pyrazines corrosion inhibitors for steel in oilfied acidizing environment. International Journal of Electrochemical Science, 15(9),9066-9080. https://doi.org/10.20964/2020.09.72.

[8] Umoren, S. A., AIAhmary, A. A., Gasem, Z. M., & Solomon, M. M. (2018). Evaluation of chitosan and carboxymethylcellulose as ecofriendly corrosion inhibitions for steel. International Journal of Biological Macromolecules.,117, 1017 – 1028. https://doi.org/10.1016/j.ijbiomac.2018.06.014.

[9] Zhao, Q., Li, L., Zhang, L., &Zhao, M. (22023). Recognition of Corrosion State of Water Pipe Inner Well Based on SMA-SVM under RFFeature Selection. Coatings, 13(1). https://doi.org/10.3390/coatings13010026.